23. *Relation between the Gravity Anomalies and the Corresponding Subterranean Mass Distribution. (III.)*

By Chuji TSUBOI,

Earthquake Research Institute.

(Read Dec. 22, 1937, Feb. 15, 1938, Jan. 17, 1939.—
Received March 20, 1939.)

1. In his earlier papers, the present writer[1] developed a direct method, with the aid of which it is possible to estimate, from the gravity anomalies that are observed in a certain region, the responsible subterranean mass distribution. It need scarcely be added that it is owing to the several physical assumptions that are made, that the solution of this problem is rendered possible, if not uniquely, notwithstanding its mathematical indeterminateness. The assumptions underlying the present method are that the gravity anomalies are caused by an undulation of the boundary surface between the crustal and the denser subcrustal materials, and that so far as the resulting gravity anomalies are concerned, this undulation is such that the inequality of the mass caused by it could be replaced by the mass concentrated at the average depth of the boundary. The fundamental principle of this method lies in the fact that, if the distributions both of gravity anomalies Δg and the responsible masses Δm, which are assumed to be concentrated on a single subterranean plane, are expressed in harmonic series of the coordinates, say ξ and η, then there is a simple mathematical relation between the corresponding harmonic coefficients of the two series.

Thus, if

$$\Delta g(\xi\eta) = \sum_m \sum_n B_{m,n} C_m(\xi) C'_n(\eta),$$

then

$$\Delta m(\xi\eta) = \frac{1}{2\pi k^2} \sum_m \sum_n B_{m,n} f(d, m, n) C_m(\xi) C'_n(\eta)$$

is one of the subterranean mass distributions that would cause these gravity anomalies. Here C_m and C'_n are orthogonal harmonic functions of the order m and n; d the assumed average depth of the subterra-

1) C. TSUBOI and T. FUCHIDA, *Bull. Earthq. Res. Inst.*, **15** (1937), 636; **16** (1938), 273. C. TSUBOI, *ibid.*, **15** (1937), 950; *Proc. Imp. Acad. Tokyo*, **14** (1938), 170.

nean boundary; f a function of d, m, and n; and k^2 the universal constant of attraction, $6{\cdot}67\times10^{-8}$ c. g. s. The practical application of the method consists, first, in developing the distribution of gravity anomalies in the region to be studied into a suitable harmonic series, second, in multiplying each of the coefficients by the numerical constants depending on the assumed average depth of the subterranean boundary, as well as on the order of harmonics, and lastly in summing up the series with these new harmonic coefficients. This last series will give the required distribution of the subteranean mass.

In the case of double Fourier series, for instance, if

$$\Delta g(xy)=\sum_m\sum_n B_{mn}\begin{matrix}\cos\\ \sin\end{matrix}mx\begin{matrix}\cos\\ \sin\end{matrix}ny\,,$$

then

$$\Delta m(xy)=\frac{1}{2\pi k^2}\sum_m\sum_n B_{mn}\exp\left(\sqrt{m^2+n^2}d\right)\begin{matrix}\cos\\ \sin\end{matrix}mx\begin{matrix}\cos\\ \sin\end{matrix}ny\,.$$

In another paper[2], a method based on a similar idea was suggested by the writer, by means of which the most probable thickness of the isostatic earth's crust is calculable directly from the observed Bouguer gravity anomalies.

T. Nagata[3] showed that the method may, with slight modification, be applied to magnetic anomalies also.

Since the publications of these articles, the writer, with the collaboration of others, has been able to avail himself of this new method in discussing actual gravity distributions measured in various parts of the world. It is the purpose of the present series of articles that are to be published in this Bulletin to describe the conclusions reached by means of these studies, and to illustrate at the same time the feasibility of this new method.

2. Eötvös's Schematic Example.

In his famous article published in 1910, R. v. Eötvös[4] showed for the first time the geophysical significance of measuring the gravity gradient along the earth's surface, and demonstrated, by means of a numerical example, the relation between the gradient and the corresponding subterranean mass distribution. In that example, he assumed that two materials of different densities are arranged in layers, their bounda-

2) C. TSUBOI, *Bull. Earthq. Res. Inst.*, **16** (1938), 285.

3) T. NAGATA, *Bull. Earthq. Res. Inst.*, **16** (1938), 550; *Imp. Acad. Proc. Tokyo*, **14** (1938), 176.

4) R. v. EÖTVÖS, *Verh.* 16 *Allg. Conf. d. Intern. Erdmessung*, (1910), 317.

ry surface varying in depth as shown in Fig. 1 and in Table I. Taking the difference in density of the two materials to be 0·8, he calculated the resulting gravity gradients $\frac{\partial g}{\partial x}$ that should be observed on the earth's surface; they are shown in Fig. 1 and in Table I.

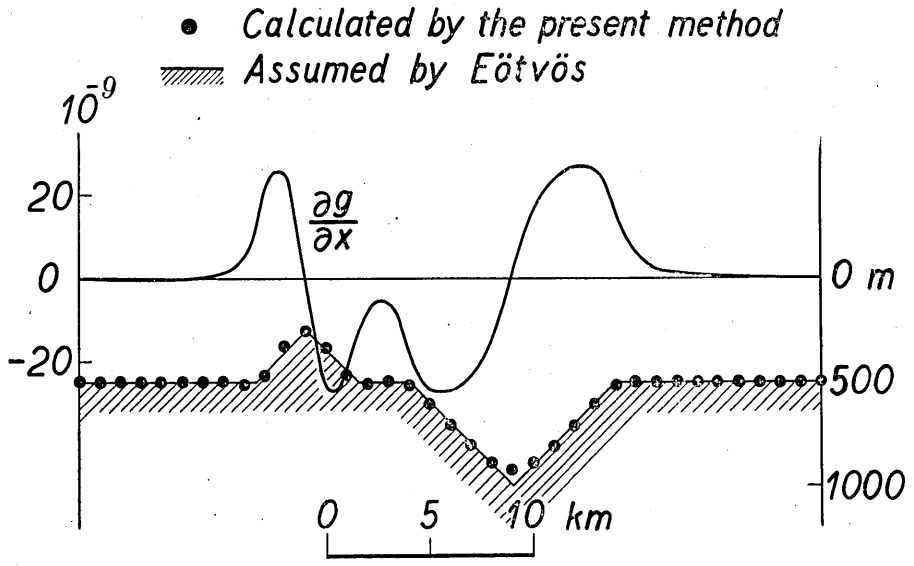

Fig. 1

Table I.

Horizontal Distance in km	Depth of the Boundary in m	Gravity Gradient in 10^{-9} c. g. s.	Calculated Relief of the Boundary in m	Calculated Depth of the Boundary in m
0	500	0	52·5	498·5
1	500	0	52·7	498·3
2	500	+0·1	53·7	497·3
3	500	+0·1	52·8	498·2
4	500	+0·2	53·3	497·7
5	500	+0·2	52·7	498·3
6	500	+0·5	50·3	500·7
7	500	+1·2	51·6	499·4
8	500	+5·2	41·8	509·2
9	450	+21·4	83·0	468·0
10	350	+25·3	217·6	333·4
11	250	− 0·5	302·1	248·9
12	350	−26·3	219·0	332·0
13	450	−22·7	83·6	467·4
14	500	− 7·2	43·6	507·4

(to be continued.)

Table I. (*continued.*)

Horizontal Distance in km	Depth of the Boundary in m	Gravity Gradient in 10^{-9} c. g. s.	Calculated Relief of the Boundary in m	Calculated Depth of the Boundary in m
15	500	− 5·7	54·0	497·0
16	500	−16·9	32·9	518·1
17	600	−26·5	− 57·1	608·1
18	700	−26·4	−161·0	712·0
19	800	−23·6	−250·8	801·8
20	900	−16·8	−338·5	889·5
21	1000	− 0·1	−380·1	931·1
22	900	−16·7	−338·5	889·5
23	800	−23·4	−250·5	801·5
24	700	−26·2	−160·9	711·9
25	600	−26·2	− 56·8	607·8
26	500	−16·2	34·3	516·7
27	500	−4·3	54·0	497·0
28	500	−1·8	50·3	500·7
29	500	−1·1	51·7	499·3
30	500	−0·7	49·6	501·4
31	500	−0·5	51·8	499·2
32	500	−0·4	49·3	501·7
33	500	−0·3	52·2	498·8
34	500	−0·2	50·5	500·5
35	500	−0·1	53·0	498·0
36	500	0	52·5	498·5

An attempt will now be made to find, from this given distribution of gravity gradients, the responsible subterranean mass distribution, regarding it as if it were unknown. Although it would not be an easy matter to do this by means of the customary trial and error method, our new method will give the answer without any difficulty.

According to the method developed in the previous paper, if

$$\frac{\partial g}{\partial x}(x)=\sum_m \gamma_m \begin{matrix}\cos\\ \sin\end{matrix} mx\,,$$

then the relief of the subterranean boundary surface that is responsible for this distribution of the gradients is given by

$$h(x)=\pm\frac{1}{2\pi k^2 \Delta\rho}\sum_m \frac{1}{m}\gamma_m \exp(md) \begin{matrix}\sin\\ \cos\end{matrix} mx\,,$$

where d is the average depth of the surface and $\Delta\rho$ the difference in

density of the two materials bounded by that surface. Taking the extent from 0 km to 36 km to be 2π, the gradient was analysed into a Fourier series, the resulting coefficients being given in Table II. Following Eötvös, if we take the average depth of the subterranean surface to be 551 m, this is equal to 0·096 in circular measure, since

$$\frac{551\times 2\pi}{36\times 10^3}=0{\cdot}096\,.$$

Then we get the values of $\frac{1}{m}\exp(md)$, given in the 4th column of Table II, which should be multiplied with each of the Fourier coefficients of $\frac{\partial g}{\partial x}$ in order to get those for h. In this way, we calculate the Fourier coefficients h_m of the relief h, which are also given in the same table. By synthesizing the series with these coefficients, we get

Table II.

m	γ_m in $\frac{36}{2\pi}\times 10^5\times 10^{-10}$		$\frac{1}{m}\exp(md)$	$\frac{\gamma_m}{m}\exp(md)$ in $\frac{36}{2\pi}\times 10^5\times 10^{-10}$	
	cos	sin		cos	sin
0	−0·1	——	——		
1	51·6	−53·2	1·101	58·6	56·9
2	−107·5	74·6	0·606	−45·2	−65·1
3	72·9	−36·8	0·445	16·4	32·4
4	−6·4	−38·4	0·367	14·1	−2·3
5	3·9	67·7	0·323	−21·9	1·2
6	−38·1	−21·9	0·297	6·5	−11·3
7	32·6	−30·9	0·280	8·7	9·1
8	8·4	30·0	0·269	−8·1	2·3
9	−29·1	0·1	0·264	0	−7·7
10	14·5	−9·6	0·261	2·5	3·8
11	2·8	−1·7	0·261	0·4	0·7
12	−4·1	6·4	0·264	−1·7	−1·1
13	−0·4	−0·9	0·268	0·2	−0·1
14	0·7	−1·1	0·274	0·3	0·2
15	−2·0	−1·4	0·281	0·4	−0·6
16	0·4	0·5	0·290	−0·2	0·1
17	−0·3	1·1	0·301	−0·3	−0·1
18	0·1		0·313		

the values that are proportional to the relief of the subterranean boundary which, in order to be expressed in m, should be mutiplied by

$$\frac{1}{2\pi\times 6{\cdot}67\times 10^{-8}\times 0{\cdot}8}\,\frac{36\times 10^{5}}{2\pi}\times 10^{-10}\times 10^{-2}=1{\cdot}712\,.$$

The calculated relief is given in Table I. In order to obtain the depth of the subterranean boundary, the values found must be subtracted from 551 m. The final values are also given in the same table. Except at the minimum of the relief, the agreement in the depths of the boundary assumed by Eötvös with those calculated by the present method is generally satisfactory as may be seen in Fig. 1. The difference at the minimum is due to the process of condensing the subterranean mass on a single plane, the process on which the present method is based.

3. African Rift Valleys.

In 1933~1934, E. C. Bullard[5], in his gravity expedition to the African Rift Valleys, measured the intensity of gravity at some 90 points. The profile from S. Tanganyika to Rukwa Rift given in his Fig. 13, includes stations 82, 81, 85, 80, 84, 83, and 79, enumerated from west to east. Since both the gravity anomaly and the topography extend with but little variation perpendicularly to the profile, our two dimensional method is applicable here also. The topography and the

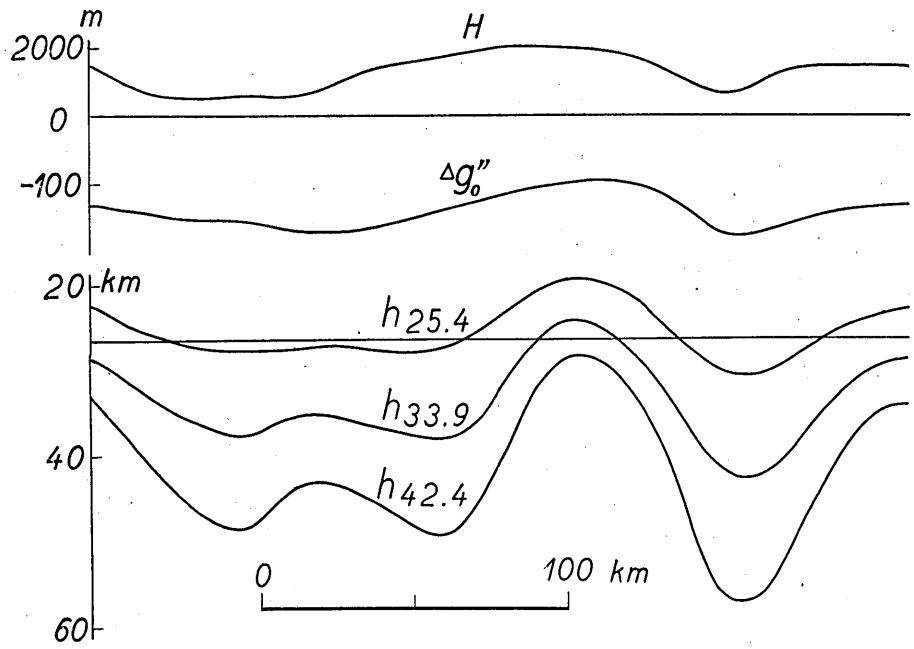

Fig. 2. African Rift Valleys.

5) E. C. BULLARD, *Phil. Trans. Roy. Soc. London*, A **235** (1936), 445.

Bouguer gravity anomaly along this profile, as given by Bullard, are reproduced here in Fig. 2.

The entire length of the profile, 266 km, which will be taken as 2π, was divided into 12 equal intervals, and the height H and the Bouguer anomaly $\Delta g_0''$ at the end of each of the intervals were read from the curves, with the results shown in Table III. In this table, the height for the lake with depth D and height of water surface H, is taken as

$$H-\frac{2\cdot7-1\cdot0}{2\cdot7}D.$$

Table III.

x	H in m	$\Delta g_0''$ in mgal	x	H in m	$\Delta g_0''$ in mgal
1	662	−142	7	2000	− 95
2	548	−153	8	1675	− 98
3	580	−168	9	750	−157
4	1275	−165	10	750	−164
5	1650	−145	11	1200	−140
6	2040	−118	12	1475	−130

The topography and the Bouguer anomaly were then analysed into Fourier series like

$$H(x)=\sum_m H_m \begin{matrix}\cos\\ \sin\end{matrix} mx,$$

$$\Delta g_0''(x)=\sum_m B_m \begin{matrix}\cos\\ \sin\end{matrix} mx,$$

with the results given in Table IV.

Table IV.*

m	H_m in m		B_m in mgal	
	cos	sin	cos	sin
0	1212		−140	
1	−499	−194	− 13	−14
2	465	− 7	18	18
3	181	−130	7	− 7
4	− 1	− 64	− 4	− 4
5	35	− 21	− 1	2
6	82		3	

The constant terms H_0 and B_0 are respectively 1212 m and −140 mgal. If the topography with this average height is supported iso-

* The values given in my previous paper are to be revised.

statically, then it must be

$$-2\pi k^2 \rho H_0 = B_0$$

where ρ is the density of the crustal material. From this, we get $\rho = 2{\cdot}76$, which is quite a reasonable value, leading to the conclusion that isostasy holds here perfectly, at any rate for this average topography. In 8 out of the remaining 11 pairs of H_m and B_m, they have the same algebraic sign, which fact suggests that the smaller topographies in this region are in a condition far removed from isostasy, as will be explained below.

If the topography in a certain region is in perfect isostatic equilibrium, and if it be expressed in a Fourier series, such as

$$H(x) = \sum_m H_m \begin{matrix}\cos \\ \sin\end{matrix} mx ,$$

then the corresponding compensating mass (in Airy's sense of isostasy) must be given by

$$M(x) = -\sum_m \rho H_m \begin{matrix}\cos \\ \sin\end{matrix} mx .$$

If this mass is at depth d from the earth's surface, the expected Bouguer anomalies are

$$\Delta g_0'(x) = -2\pi k^2 \sum_m \rho H_m \exp(-md) \begin{matrix}\cos \\ \sin\end{matrix} mx .$$

In order that this shall be equal to the observed anomalies

$$\Delta g_0''(x) = \sum_m B_m \begin{matrix}\cos \\ \sin\end{matrix} mx ,$$

we must have

$$-2\pi k^2 \rho H_m \exp(-md) = B_m .$$

One of the necessary conditions for isostasy, therefore, is that H_m and B_m of the same order shall differ in algebraic sign. In the present case of the African Rift Valleys, this requirement is not fulfilled. That in most pairs, H_m and B_m have the same algebraic sign in this case, indicates that the boundary surface between the crustal and subcrustal materials has a shape similar to the surface topography. We have seen, on the other hand that, in accordance with the requirements of isostasy, the constant terms H_0 and B_0 differ in algebraic sign. From these considerations, we conclude that the section of the earth's crust across the Rift Valleys, roughly, is like that schematically shown in Fig. 3.

For more detailed information, further numerical calculations are needed. If d is the average depth of the boundary surface between the crustal and subcrustal materials, then the Bouguer gravity anomalies that are observed along the earth's surface may be explained by assuming that the relief of the boundary is such as given by

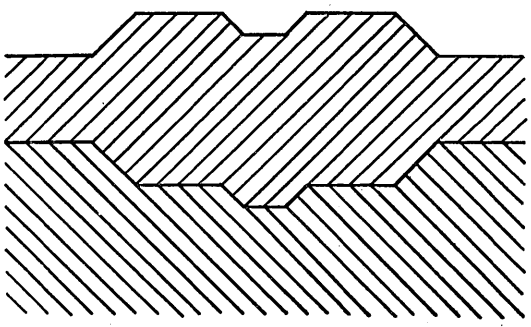

Fig. 3. Schematic Section of the African Rift Valleys.

$$h(x)=\frac{1}{2\pi k^2 \Delta\rho}\sum_m B_m \exp(md)\begin{matrix}\cos\\ \sin\end{matrix} mx\,.$$

In order to get h, the value of d will be assumed to be successively 0·6, 0·8, and 1·0, corresponding respectively to 25·4, 33·9, and 42·4 km in actual length, because in this case 266 km was taken to be 2π. Putting $\Delta\rho=0{\cdot}6$, and omitting orders higher than 4, the series for h were synthesized with the results given in Table V. They are also graphical-

Table V.

x	d=25·4 km		d=33·9 km		d=42·4 km	
	Relief h in km	Depth (d-h) in km	h	d-h	h	d-h
0	3·1	22·3	5·5	28·4	9·5	32·9
1	0·2	25·2	0·2	33·7	0·3	42·1
2	−2·2	27·6	−3·4	37·3	−5·7	48·1
3	−1·7	27·1	−1·7	35·6	−1·2	43·6
4	−2·0	27·4	−2·3	36·2	−2·2	44·6
5	−2·3	27·7	−4·0	37·9	−6·7	49·1
6	1·6	23·8	1·6	32·3	1·1	41·3
7	6·3	19·1	9·5	24·4	14·4	28·0
8	3·9	21·5	6·0	27·9	9·6	32·8
9	−3·1	28·5	−5·4	39·3	−9·4	51·8
10	−4·5	29·9	−7·4	41·3	−12·2	54·6
11	0·5	24·9	1·4	32·5	3·2	39·2
12	3·1	22·3	5·5	28·4	9·5	32·9

ly shown in Fig. 2. The reliefs of the earth's surface and the subterranean boundary are almost similar in shape, whatever the depth

assumed. This fact, which has already been pointed out by Bullard from an indirect method, has a very important bearing on the mechanism of formation of the characteristic topography of the Rift Valleys.

4. The Central Part of Honsyû, the Main Island of Japan.

The area to be studied, as will be seen from Fig. 4, is a rectangular one, 350×200 km^2. Table VI is a list of the name[6], longitude, latitude, height, and Bouguer anomaly of and at the stations included in this area, arranged according to longitude.

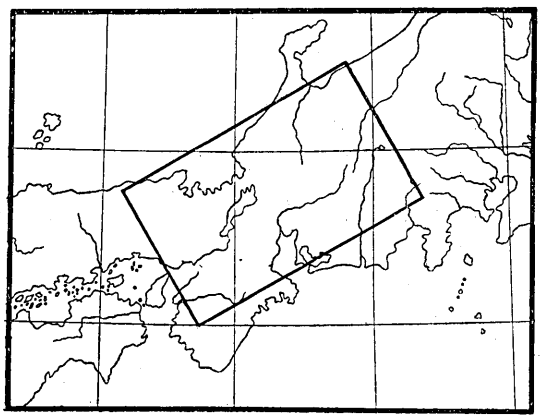

Fig. 4.

Figs. 5 and 6 show the contour lines for the topographies and the Bouguer anomalies. In drawing the contour lines in these figures, the values

Table VI

Name	λ	φ	H in m	$\Delta g_0''$ in mgal
1. Hukutiyama	135° 9′ E	35° 18′ N	37	−27
2. Mikage	135 15	34 43	5	− 8
3. Kyôto	135 47	35 2	55	− 2
4. Nara	135 51	34 41	97	−33
5. Turuga	136 3	35 39	3	− 6
6. Ueno	136 8	34 46	158	−41
7. Hikone	136 15	35 16	92	−29
8. Hukui	136 15	36 3	11	−42
9. Kanazawa	136 42	36 33	24	−20
10. Gihu	136 46	35 26	14	− 5
11. Nagoya	136 53	35 10	14	−14
12. Okazaki	137 10	34 57	25	−43
13. Toyama	137 13	36 40	8	−63
14. Takayama	137 16	36 9	558	−19
15. Nakatugawa	137 32	35 29	339	− 2
16. Matumoto	137 59	36 14	591	−43
17. Kamisuwa	138 8	36 2	779	−30
18. Kôhu	138 35	35 39	270	−12

6) E. BORRAS; *Verh. 6 Allg. Conf. d. Intern. Erdmessung*, III Teil, (1911).

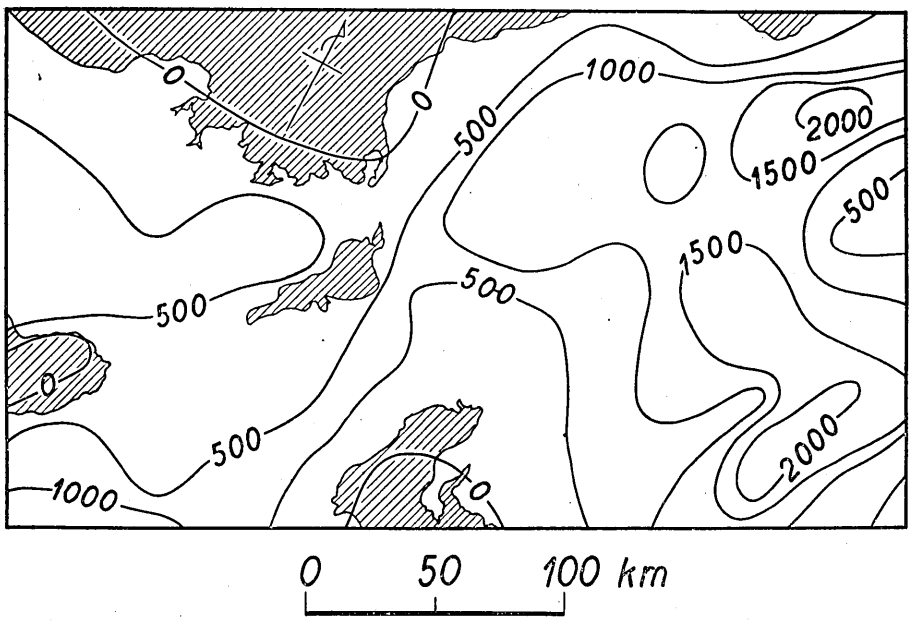

Fig. 5. Height in Central Part of Honsyû (m).

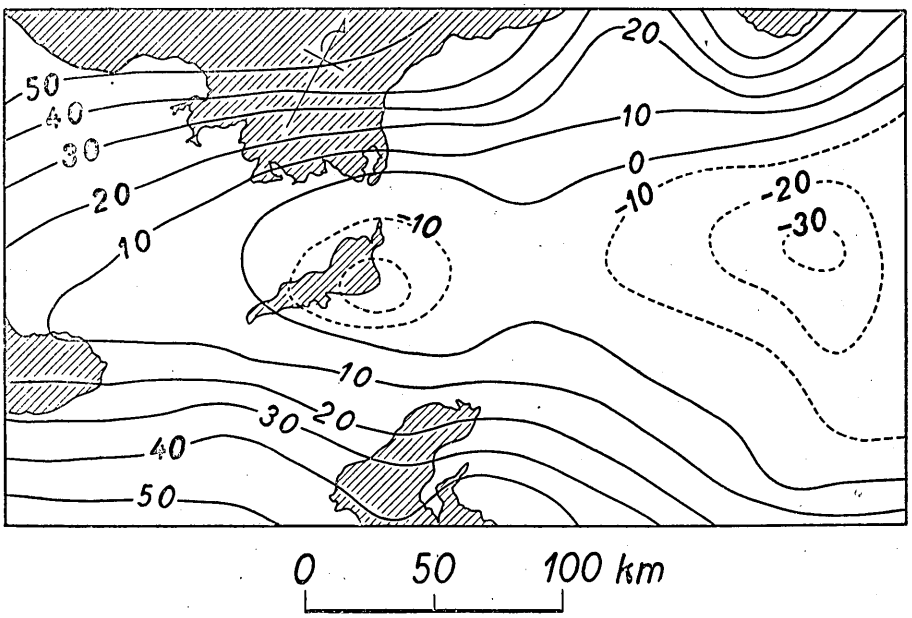

Fig. 6. $\Delta g''_0$ in Central Part of Honsyû (mgal).

for stations outside the area were also taken into account. The area was then divided into 12×12 small equal rectangles by series of lines parallel to the sides, which will hereinafter be referred to as the x- and y-directions. The heights and the Bouguer anomalies at 144 points of intersection of the lines were read off by means of interpolations. Where the point of intersection of the series of parallel lines fell on a volcano, the height of its base was taken, instead of the height itself. Tables VII and VIII give these readings.

Table VII.

H in m.

y \ x	1	2	3	4	5	6	7	8	9	10	11	12
1	450	−100	−100	−200	−150	50	400	900	500	60	700	760
2	250	500	−100	−100	−100	100	1100	1100	1300	1500	2200	1850
3	400	400	180	−100	−100	300	1000	1400	900	1600	1900	500
4	750	300	480	300	400	1000	1200	1000	800	1500	650	500
5	550	450	700	600	400	1100	1300	1100	1350	1300	500	300
6	300	700	750	500	100	800	1000	700	1500	1800	850	630
7	550	500	350	200	600	50	500	600	1500	1600	1250	1500
8	−100	50	400	200	1000	10	250	900	1200	1700	1600	1450
9	30	350	400	250	100	50	200	750	1350	750	2750	1600
10	700	100	500	700	40	50	200	750	600	2000	1700	900
11	900	350	850	300	−100	−100	300	900	1100	2400	900	1200
12	1100	1600	1200	300	−100	−100	100	580	1350	1400	800	1000

Table VIII.

$\Delta g_0''$ in mgal.

y \ x	1	2	3	4	5	6	7	8	9	10	11	12
1	55	55	54	52	50	45	40	16	20	50	25	10
2	45	43	41	40	41	41	25	11	18	21	18	− 3
3	33	30	25	20	19	19	10	5	5	2	− 4	−15
4	25	21	11	2	− 2	0	3	− 2	−19	−18	−20	−17
5	19	10	4	− 6	−11	− 6	−2	− 9	−18	−24	−30	− 15
6	12	6	1	−11	−22	−10	−5	−10	−17	−23	−30	−15
7	8	5	2	−10	−20	− 5	−2	− 5	−10	−13	−25	−15
8	16	13	11	5	2	0	4	0	− 5	− 8	−20	−14
9	26	27	30	19	13	12	15	9	− 2	− 5	−14	−13
10	35	38	42	38	20	24	28	17	7	− 1	−10	−10
11	44	49	48	41	31	41	40	28	17	7	0	0
12	56	57	54	46	40	47	46	36	26	17	12	15

Both quantities were then analysed into double Fourier series, like

$$H(xy) = \sum_m \sum_n H_{mn} \begin{matrix}\cos\\ \sin\end{matrix} mx \begin{matrix}\cos\\ \sin\end{matrix} ny ,$$

$$\Delta g_0''(xy) = \sum_m \sum_n B_{mn} \begin{matrix}\cos\\ \sin\end{matrix} mx \begin{matrix}\cos\\ \sin\end{matrix} ny ,$$

the coefficients found being tabulated in Tables IX and X.

Table IX.

H_{mn} in m

cos − cos

n \ m	0	1	2	3	4	5	6
0	711	331	−118	− 4	42	43	7
1	−82	240	− 47	75	− 5	−42	14
2	− 3	−65	−110	−99	37	59	30
3	−10	−45	40	−20	−55	32	−15
4	35	75	− 42	−60	−26	−51	−13
5	76	86	− 60	−17	23	9	−11
6	43	12	− 54	−45	27	35	17

cos − sin

n \ m	0	1	2	3	4	5	6
1	−21	−191	117	−74	−114	−41	4
2	−61	110	172	121	− 22	94	−31
3	−71	−122	73	73	59	−75	−27
4	−88	− 28	− 13	8	34	−66	−12
5	−58	− 98	−104	−15	− 8	−44	6

sin − cos

n \ m	1	2	3	4	5
0	−459	−110	−106	3	35
1	50	58	− 21	−27	23
2	174	139	138	142	18
3	112	42	90	−33	77
4	31	31	− 70	−80	−104
5	41	11	10	−30	− 74
6	23	−29	0	28	19

sin--sin

n \ m	1	2	3	4	5
1	−55	236	−33	138	− 12
2	−81	−31	5	−103	−105
3	67	49	−21	− 74	− 94
4	86	37	27	− 61	8
5	20	−13	12	− 66	76

Table X.

B_{mn} in mgal

cos−cos

n \ m	0	1	2	3	4	5	6
0	12·39	− 5·03	− 3·66	− 4·54	− 2·73	− 2·92	− 1·23
1	24·07	− 4·61	− 1·92	− 2·73	− 0·83	− 0·99	− 0·63
2	− 0·02	1·18	0·63	0·47	1·50	0·78	0·65
3	− 0·07	0·33	0·80	0·68	− 0·55	0·65	0·18
4	1·42	0·06	− 0·14	0·67	0·43	− 0·23	− 0·12
5	0·00	− 0·42	0·57	0·80	0·33	− 0·47	− 0·11
6	− 0·09	− 0·10	0·53	0·66	− 0·35	− 0·23	− 0·05

cos−sin

n \ m	0	1	2	3	4	5	6
1	2·43	1·70	1·11	− 2·24	− 0·62	− 0·85	− 0·46
2	3·15	1·49	− 0·01	− 2·05	0·03	0·42	− 0·06
3	1·25	0·83	− 0·35	− 0·43	− 0·22	0·93	− 0·12
4	− 0·03	0·91	−1·14	−0·38	− 0·03	0·32	0·41
5	0·18	0·08	−0·71	0·01	− 0·05	0·39	0·00

sin−cos

n \ m	1	2	3	4	5
0	13·02	8·70	1·80	3·68	1·32
1	3·62	− 2·88	− 0·26	0·41	− 0·35
2	− 1·25	1·78	− 0·65	0·81	− 0·11
3	− 0·35	1·35	0·25	− 0·60	0·50
4	0·03	1·21	0·25	− 0·63	− 0·04
5	− 0·27	0·93	0·26	− 0·46	− 0·40
6	0·28	0·53	0·05	− 0·31	− 0·32

sin−sin

n \ m	1	2	3	4	5
1	0·58	−2·25	1·02	−0·31	0·05
2	−2·28	−4·29	−0·95	0·36	0·30
3	1·22	−1·33	−0·08	0·75	0·77
4	−0·12	−0·22	0·32	0·79	0·45
5	0·09	−0·78	0.55	0·71	0·02

The constant terms for H and $\Delta g_0''$ are respectively 711 m and 12·4 mgal. That they shall be both positive is far from the requirements of isostasy. On the other hand, the harmonic coefficients for H and $\Delta g_0''$ for the lower orders differ in algebraic sign, in qualitative agreement with the same requirements. This state of things is contrary to what was found in the case of the African Rift Valleys, where it was the constant terms for H and $\Delta g_0''$ that differed in algebraic sign, and where it was the other harmonic coefficients that were the same.

Although there are many possible explanations for this remarkable contrast, as pointed out before[7], one is that the Helmert formula of 1901, which gives the normal gravity, and from which the Bouguer anomalies were calculated, does not fit in with the gravity values observed in Japan. According to the new formula that was determined in order to better fit with the observed gravities in Japan, the normal gravity for the average latitude of the area now in question is approximately 40 mgal greater than the same as calculated from the Helmert formula. Since this means that the anomaly calculated from the new formula is 40 mgal smaller than that calculated from the Helmert formula, the constant term for $\Delta g_0''$ becomes

$$12{\cdot}4-40{\cdot}0=-27{\cdot}6 \text{ mgal}$$

which is now of opposite sign to H_0.

In 79 (55%) out of the remaining 143 pairs of harmonic coefficients H_{mn} and B_{mn}, they differ in algebraic sign, not pointing to any predominance of pairs of this kind. Fig. 7 is a diagram showing the distribution of the pairs in which H_{mn} and B_{mn} have the opposite algebraic sign, arranged according to m and n. In this figure, a small square determined by a certain combination of m and n is subdivided

7) C. TSUBOI, *Bull. Earthq. Res. Inst.*, **11** (1933), 632; C. TSUBOI and T. FUCHIDA, *ibid.*, **13** (1935), 555.

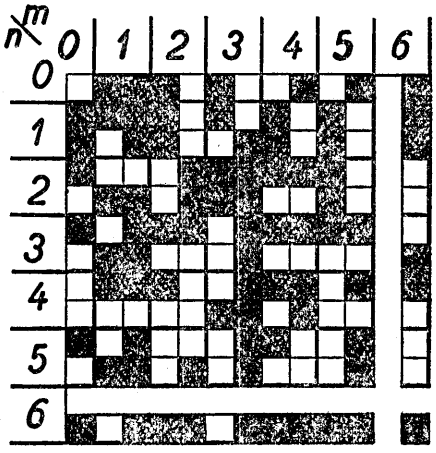

Fig. 7.

sin—sin	cos—sin
sin—cos	cos—cos

Fig. 8.

into four small squares which will be called the domains of sin—sin, sin—cos, cos—sin, and cos—cos (see Fig. 8). If in a pair of the harmonic coefficients H_{mn} and B_{mn} of a certain m n, they differ in algebraic sign, then the corresponding small domain of the square determined by that m n is made black. In Fig. 7, the black domains are likely to predominate towards where m and n are smaller. From the physical point of view, this is quite natural, since the dependence of the predominance on the order of the harmonics implies dependence on the horizontal extent of the topography. This is known as the problem of local versus regional isostasy. In order to ascertain this eventual relation, the percentage

$$\frac{\text{Number of pairs in which } H_{mn} \text{ and } B_{mn} \text{ have opposite algebraic sign}}{\text{Total number of pairs of the order } \sqrt{m^2+n^2}}$$

was calculated for each $\sqrt{m^2+n^2}$ separately. In doing this, it must be carefully borne in mind that the form of the area now under study is not square. Since the area is a rectangle, with the ratio of the sides

$$200\,\text{km} : 350\,\text{km} = 1 : 1{\cdot}75,$$

the wave-length of the n-th harmonics in the y-direction is the same as that of the 1·75 n-th harmonics in the x-direction. Therefore, if referred to the x-direction alone, $\sqrt{m^2+n^2}$ becomes as shown in Table XI.

Table XI.

n \ m	0	1	2	3	4	5	6
0	0	1·00	2·00	3·00	4·00	5·00	6·00
1	1·75	2·01	2·66	3·47	4·37	5·30	6·25
2	3·50	3·64	4·03	4·61	5·32	6·10	6·95
3	5·25	5·34	5·62	6·05	6·60	7·25	7·32
4	7·00	7·07	7·28	7·62	8·06	8·60	9·22
5	8·75	8·81	8·98	9·25	9·62	10·08	10·61
6	10·50	10·55	10·69	10·92	11·24	11·63	12·09

The total number of pairs, and those in which H_{mn} and B_{mn} have opposite algebraic sign, are given in Table XII according to $\sqrt{m^2+n'^2}$.

Table XII.

$\sqrt{m^2+n'^2}$	0	−1	−2	−3	−4	−5	−6	−7	−8	−9	−10	−11	−12	−13	Total
Total Number of Pairs	1	4	10	12	14	20	17	20	18	10	13	4	4		144
Number of Pairs in which H_{mn} and B_{mn} have Opposite Sign	0	4	6	6	9	11	9	9	9	4	7	4	1		79
Percentage	0	100	60	50	64	55	53	45	50	40	54	100	25		55

It is notable that the percentage decreases asymptotically, from 100, down to 50 as the order $\sqrt{m^2+n'^2}$ increases. If we take $\sqrt{m^2+n'^2}=3$ as the threshold value of $\sqrt{m^2+n'^2}$, beyond which the percentage is 50, this corresponds to the square

$$\left[\frac{350}{\sqrt{3^2/2}}\right]^2=[165\text{ km}]^2$$

provided $m=n'$. This implies that topographies smaller than a quarter of this square are supported by the mechanical strength of the earth's crust, and those larger than this, isostatically. By assuming that these larger topographies are in perfect isostasy, it is possible to calculate the thickness of the earth's crust d by means of the relation

$$-2\pi k^2\rho H_{mn}\exp(-\sqrt{m^2+n^2}d)=B_{mn}.$$

Table XIII.

$\sqrt{m^2+n^2}$	1—2		2—3		3—4		4—5		5—6		6—7		7—8		8—9		9—10		10—11		11—12		12—13	
	H_{mn} m	B_{mn} mgal	H_{mn}	B_{mn}	H_{mn}	B_{mn}	H_{mn}	B_{mn}	H_{mn}	B_{mn}	H_{mn}	B_{mn}	H_{mn}	B_{mn}	H_{mn}	B_{mn}	H_{mn}	B_{mn}	H_{mn}	B_{mn}	H_{mn}	B_{mn}	H_{mn}	B_{mn}
	− 82	24·1	240	−4·6	− 65	1·2	−110	0·6	− 45	0·3	− 20	0·7	−60	0·7	86	−0·4	−17	0·8	43	−0·1	27	−0·4	17	−0·1
	331	−5·0	−191	1·7	75	−2·7	− 99	0·5	43	−2·9	7	−1·2	−15	0·2	−60	0·6	−15	0	12	−0·1	35	−0·2		
	− 21	2·4	−110	8·7	− 61	3·2	42	−2·7	− 71	1·3	14	−0·6	−28	0·9	−26	0·4	−12	0·4	−54	0·5	28	−0·3		
	−459	13·0	58	−2·9	174	−1·3	172	0	−122	0·3	73	−0·4	8	−0·4	−58	0·2	−66	0·7	−45	0·7	19	−0·3		
			− 55	0·6	−106	1·8	121	−2·1	73	−0·4	59	−0·2	−75	0·9	−98	0·1			9	−0·5				
			236	−2·3	− 33	1·0	138	−0·7	− 22	0	4	−0·5	−70	0·3	34	0			−44	0·4				
							− 27	0·4	112	−0·4	18	−0·1	86	−0·1	−66	0·3			−29	0·5				
							5	−1·0	23	−0·4	− 74	0·8	37	−0·2	41	−0·3								
							138	−0·3	49	−1·3	−105	0·3	−94	0·8	−61	0 8								
									−103	0·4														
									− 12	0·1														
Most probable d in circular measure.	0·89		0·72		0·55		0·65		0·48		0·44		0·36		0·36		0·23		0·23		0·21		0·23	
Most probable d in km.	50		40		31		36		27		25		20		20		13		13		12		13	

Now, in Table XIII, we have a number of pairs of B_{mn} and H_{mn} for determining d, together with the most probable d calculated separately from each $\sqrt{m^2+n'^2}$. In the table, the coefficients of higher orders are also treated similarly, notwithstanding their slight physical significance.

The pairs of harmonics of the lower orders yield a very reasonable value of 50~40 km for the thickness of the earth's crust. The depth of compensation in Pratt's sense is twice this thickness[8], i.e. 100~80 km. Although there is likely to be a marked tendency for d to decrease with increase in $\sqrt{m^2+n'^2}$, much weight cannot be placed on this fact because of inaccuracy in the harmonic coefficients of the higher orders that were used in the calculations.

From the fact that the constant term for $\Delta g_0''$ was 12 mgal, the thickness of the isostatic earth's crust for zero height would be slightly smaller than the value found here.

5. Dutch East Indies.

In this section, a study will be made of the gravity anomalies that Vening Meinesz[9] found in the Dutch East Indies during his submarine expedition there. The profiles Nos. 21~13 of Meinesz shown here in Fig. 9 will be discussed by means of our two dimensional method. The whole length of each profile was divided into 12 equal intervals, and the Bouguer anomaly $\Delta g_0''$, the height H, and the reduced height H' at the ends of the intervals were read by means of interpolations, with the results shown in Table XIV. Here the reduced height means the effective height. Should the sea water be replaced bycrustal material having the same mass. It is given by

$$H'=H-\frac{1\cdot03}{2\cdot7}H=0\cdot62H\,,$$

if H is negative, and by

$$H'=H$$

if H is positive.

Before expanding the gravity anomaly and the height along the 9 profiles into Fourier series, tests were made of the practical method of

8) H. JEFFREYS, *Gerl. Beitr. z. Geophys.*, **15** (1926), 167.

9) VENING MEINESZ, *Gravity Expedition at Sea*, 1923~1932. II (1934), Delft.

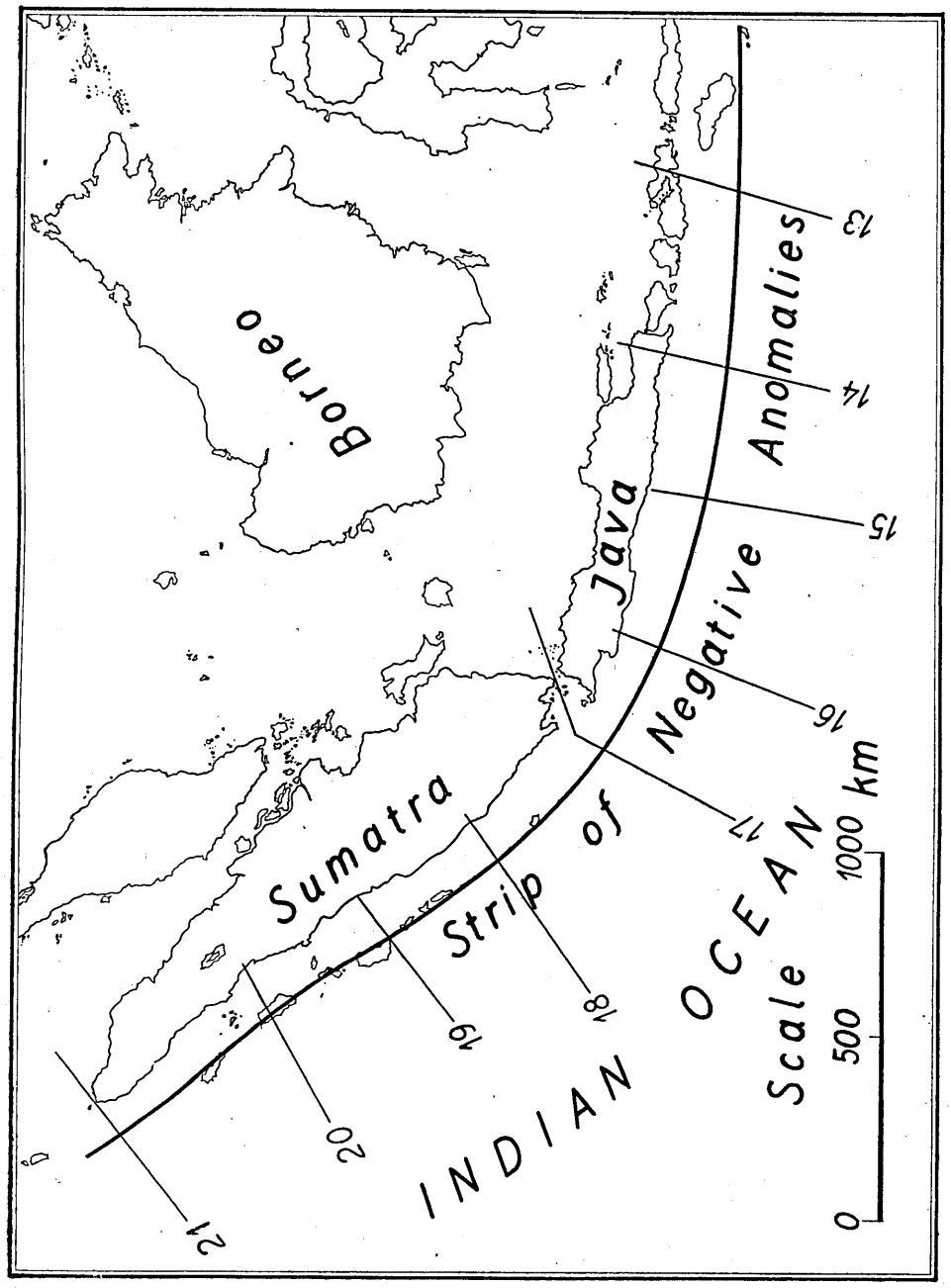

Fig. 9.
Dutch East Indies.

Table XIV.

$\Delta g_0''$ in mgal; H and H' in 10 m.

Profile	21			20			19			18		
Total length in km	600			480			420			600		
x	$\Delta g_0''$ in mgal	H in 10 m	H' in 10 m	$\Delta g_0''$ in mgal	H in 10 m	H' in 10 m	$\Delta g_0''$ in mgal	H in 10 m	H' in 10 m	$\Delta g_0''$ in mgal	H in 10 m	H' in 10 m
0	66	−130	− 81	−15	60	60	−4	0	0	45	20	20
1	88	−130	− 81	14	− 10	− 6	16	− 48	− 30	25	− 20	− 12
2	91	−124	− 77	10	− 30	− 19	34	−144	− 89	10	−110	− 68
3	70	− 35	− 22	− 9	− 54	− 33	37	−160	− 99	34	− 18	− 11
4	25	− 13	− 8	26	13	13	38	− 8	− 5	190	−214	−133
5	0	−144	− 89	127	− 60	− 37	50	− 67	− 42	304	−544	−337
6	18	−290	−180	219	−479	−297	93	−220	−136	330	−558	−346
7	70	−275	−171	272	−520	−322	1 0	−460	−285	335	−544	−337
8	135	−260	−161	305	−498	−309	278	−560	−347	335	−498	−309
9	185	−419	−260	320	−480	−298	320	−510	−316	326	−472	−293
10	226	−437	−271	318	−469	−291	340	−460	−285	324	−519	−322
11	250	−437	−271	310	−469	−291	330	−430	−267	320	−570	−353
12	252	−439	−272	298	−469	−291	302	−430	−267	313	−580	−360

(*continued.*)

17			16			15			14			13		
840			600			600			600			540		
$\Delta g_0''$ in mgal	H in 10 m	H' in 10 m	$\Delta g_0''$ in mgal	H in 10 m	H' in 10 m	$\Delta g_0''$ in mgal	H in 10 m	H' in 10 m	$\Delta g_0''$ in mgal	H in 10 m	H' in 10 m	$\Delta g_0''$ in mgal	H in 10 m	H' in 10 m
24	− 5	− 3	140	30	30	100	− 15	− 9	3	110	110	105	−340	−211
33	− 5	− 3	100	−228	−141	145	−220	−136	65	15	15	110	−110	− 68
28	− 5	− 3	50	−310	−192	130	−349	−216	155	−210	−130	78	60	60
28	− 5	− 3	70	−312	−193	54	−178	−110	161	−290	−180	95	−120	− 74
58	− 40	− 25	254	−500	−310	140	−360	−223	128	−330	−205	125	−230	−143
110	−100	− 62	338	−640	−397	265	−685	−425	103	−280	−174	135	−265	−164
70	−253	−157	342	−535	−332	315	−530	−329	180	−600	−372	108	−417	−259
120	−360	−223	334	−430	−267	320	−470	−291	270	−550	−341	118	−390	−242
320	−650	−403	330	−450	−279	305	−445	−276	275	−460	−285	245	−400	−248
355	−560	−347	328	−530	−329	283	−435	−270	245	− 96	−246	314	−585	−363
360	−538	−334	324	−525	−325	255	−430	−267	260	−404	−250	350	−590	−366
350	−525	−326	322	−520	−322	230	−430	−267	294	−430	−267	355	−580	−360
320	−514	−319	316	−520	−322	200	−430	−267	328	−430	−267	353	−550	−341

expansion, with special reference to profile No. 21. Three different kinds of Fourier expansion were tried, viz. (1) expansion into a cosine-series by taking the total distance of the profile as π, beyond which the symmetric profile is added; (2) expansion into a sine-series by taking the total distance as π, as before, beyond which the antisymmetric profile is added, and (3) expansion into a cos-sin-series taking the total distance as π, as before, beyond which the same profile is added, as

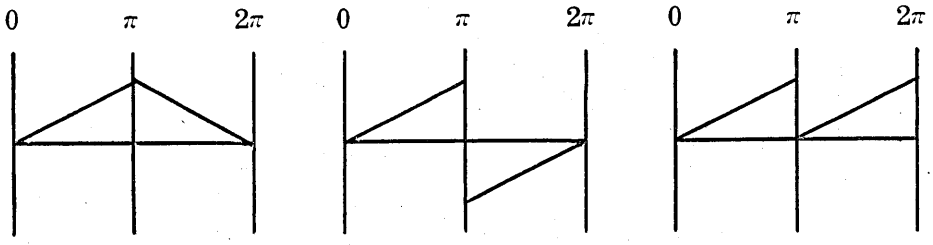

(1) Symmetric (2) Antisymmetric (3) Repeating

Fig. 10.

schematically shown in Fig. 10. These three profiles, each with a total length of 2 π, were analysed into Fourier series with the results given in Table XV.

Table XV.

B_m in mgal.

m	Symmetric		Antisymmetric		Repeating	
	cos	sin	cos	sin	cos	sin
0	109·7	0	0	0	109·7	0
1	−86·8	0	0	108·4	0	0
2	75·3	0	0	−73·9	75·3	−73·9
3	5·5	0	0	111·5	0	0
4	−18·8	0	0	−16·9	−18·8	−16·9
5	− 9·9	0	0	33·7	0	0
6	− 2·7	0	0	−19·5	− 2·7	−19·5
7	− 0·5	0	0	21·1	0	0
8	− 1·8	0	0	− 9·7	− 1·8	− 9·7
9	0·1	0	0	11·8	0	0
10	− 2·1	0	0	− 3·1	− 2·1	− 3·1
11	− 1·5	0	0	3 4	0	0
12	− 0·8	0	0	0	− 0·8	0

The corresponding subterranean mass was then calculated for each profile with the assumed depth of $d=0{\cdot}189$. Since

$$\pi = 600 \text{ km},$$

this depth is

$$d = \frac{600}{\pi} \times 0{\cdot}189 = 36 \text{ km}.$$

The results of the calculations are shown in Table XVI and in Fig. 11.

Table XVI.

Subterranean Mass in 10^4 c.g.s.

x	Symmetric	Antisymmetric	Repeating
0	2·08	0	33·99
1	28·30	45·29	2·99
2	25·21	28·49	27·32
3	22·39	27·01	19·81
4	− 3·01	0·29	− 2·92
5	−14·24	−11·09	−15·22
6	− 7·79	− 4·85	− 7·79
7	11·38	16·47	12·33
8	36·45	39·53	36·35
9	48·78	58·56	51·36
10	62·21	61·28	60·11
11	71·10	138·74	96·44
12	65·89	0	33·99

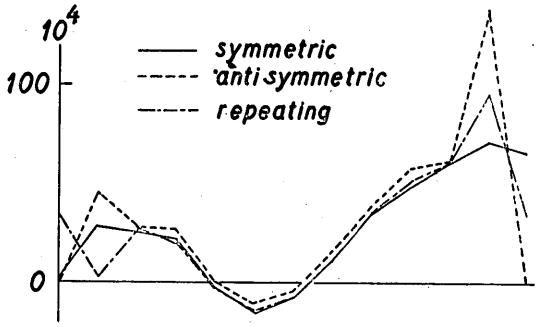

Fig. 11.

Judging from these results shown in Fig. 11, the first expansion with the addition of the symmetric profile is likely to be the most reasonable. Consequently, the Bouguer anomaly and the reduced height along all the profiles Nos. 21~13 were expanded similarly into cosine-series like

$$\Delta g_0'' = \sum_m B_m \cos mx,$$

$$H' = \sum_m H'_m \cos mx,$$

the results being given in Table XVII.

From Table XVII, it is notable that the constant and the first terms for H' and $\Delta g_0''$ have opposite algebraic signs for all the 13 profiles. This undoubtedly indicates that isostasy does prevail in this part of the world, although the isostatic anomalies may not be very small. It seems to be often erroneously stated that large isostatic anomalies in a certain region imply that the mechanism of isostasy does not exist at all in that region. It is surprising, how, even in geophysically disturbed regions of the world, such as the Dutch East Indies and Japan, the theory of isostasy is potent in diminishing the gravity anomalies. Without taking the theory into account, the anomalies would have been at least a few times larger.

Table XVII.

B_m in mgal; H'_m in m.

Profile	21		20		19		18		17		16		15		14		13	
m	B_m	H'_m	B_m	H'_m	B_m	H'_m	B_m	H'_m	B_m	H'_m	B_m	H'_m	B_m	H'_m	B_m	H'_m	B_m	H'_m
0	109·7	−1473	171·1	−1546	155·4	−1696	226·0	−2243	167·0	−1706	251·7	−2694	216·0	−2457	200·1	−2095	188·5	−2086
1	− 86·8	1138	−186·5	1723	−179·2	1532	−163·0	1711	−184·4	2051	−126·5	855	− 83·2	674	−108·5	1158	−134·4	1655
2	75·3	− 276	− 24·0	255	30·9	23	− 83·5	783	39·9	6	− 72·6	660	− 62·8	783	− 3·4	960	55·6	11
3	5·5	− 249	41·4	− 306	26·2	− 611	5·1	93	21·4	− 581	1·8	551	42·6	250	0	239	−5·7	− 155
4	− 18·8	− 203	13·6	− 313	− 28·7	327	35·3	− 526	− 36·3	179	40·0	56	32·2	− 259	− 17·3	45	−18·7	− 278
5	− 9·9	− 60	− 2·2	313	− 2·5	462	27·6	− 88	24·7	94	40·0	− 216	10·4	− 162	− 51·1	520	26·6	− 508
6	− 2·7	304	− 12·4	576	− 0·3	40	6·7	207	15·3	− 158	16·0	190	− 17·5	292	− 4·4	306	10·5	− 170
7	− 0·5	73	− 7·5	− 226	− 0·2	− 14	− 5·8	282	− 21·8	107	− 2·9	367	− 18·5	533	2·7	− 105	− 9·4	− 330
8	− 1·8	− 123	− 3·3	− 303	− 5·7	− 17	− 8·8	193	− 10·8	36	− 9·7	194	− 15·5	339	− 3·9	− 97	− 2·0	− 344
9	0·1	57	− 0·6	318	2·8	− 86	− 1·5	− 46	16·7	− 152	− 5·8	139	− 4·3	3	− 5·2	123	4·4	22
10	− 2·1	− 11	− 2·3	76	− 2·6	− 58	1·4	− 109	− 4·3	133	− 0·4	80	− 2·2	− 120	0·6	201	− 5·6	74
11	− 1·5	− 55	− 1·1	−66	− 0·2	47	3·5	− 51	− 4·4	61	5·4	64	2·9	− 9	− 0·5	− 50	− 5·4	− 34
12	− 0·8	17	− 1·2	99	− 0·1	36	2·0	− 4	1·0	− 99	3·0	54	− 0·2	42	2·2	− 106	0·7	33

From the 13 pairs of H'_0 and B_0, the density of the earth's crust can be determined by means of the relation

$$-2\pi k^2 \rho H'_0 = B_0 .$$

The least square calculations gave $\rho = 2{\cdot}24$, which differs from the value of 2·67 adopted by Meinesz in his gravity reductions, and also from 2·7 that was used in the present article in getting the effective height H' from H. If isostasy is accepted, the value ρ assumed in the reductions should have been such that H'_0 and B_0 derived from that assumed value would yield the same ρ through the relation

$$-2\pi k^2 \rho H'_0 = B_0 .$$

Since the actual length of 2π differs from one profile to another, the wave-length of the n-th order of a certain profile will be that of the m-th order of another profile. In what follows, profile No. 17 will be taken as standard, and if the orders of the harmonics of the other profiles are referred to this standard, they will be as those shown in Table XVIII.

Table XVIII.

Profile / m	14; 15; 16; 18; 21.	20	19	17	13
1	1·4	1·8	2·0	1·0	1·4
2	2·8	3·5	4·0	2·0	2·8
3	4·2	5·3	6·0	3·0	4·3
4	5·6	7·0	8·0	4·0	5·7
5	7·0	8·8	10·0	5·0	7·1
6	8·4	10·5	12·0	6·0	8·5
7	9·8	12·3	14·0	7·0	9·9
8	11·2	14·0	16·0	8·0	11·4
9	12·6	15·8	18·0	9·0	12·8
10	14·0	17·5	20·0	10·0	14·2
11	15·4	19 3	22·0	11·0	15·6
12	16·8	21·0	24·0	12·0	17·1

In 71 (66%) out of the 108 pairs of harmonic coefficients B_m and H'_m, they have opposite algebraic signs, showing unmistakable predominance of pairs of this kind over those that are not. Table XIX gives the total number of pairs, the number of pairs in which B_m and H'_m have opposite signs, and its percentage, arranged according to the order of the harmonics.

Table XIX.

m	Total Number of Pairs	Number of Pairs in which H'_m and B_m have Opposite Sign	Percentage	
1—3	16	14	88	69
3—5	10	4	40	50
5—7	10	6	60	78
7—9	17	15	88	85
9—11	10	8	80	69
11—13	16	10	63	58
13—15	8	4	50	38
15—17	13	4	31	38
17—19	3	2	67	60
19—21	2	1	50	75
21—23	2	2	100	100
23—25	1	1	100	
Sum	108	71	66	

The decrease in percentage with increase of order is again noteworthy. The percentage tends, asymptotically, down to 50 with increase in order, neglecting rather larger fluctuations due to scantiness of data. If we take $m=14$ as the order beyond which the percentage is 50, this corresponds to

$$1680\text{ km} \div 14 = 120\text{ km}.$$

Therefore, it is likely that topographies smaller than half this are supported by a mechanism other than isostasy. Athough it is rather arbitrary which m is to be taken as the threshold value, that of 120 km found here does not differ much from the 165 km found for the central part of Honsyû. This conclusion is very important in connection with the problem of regional versus local isostasy.

Now, for the determination of the thickness of the isostatic earth's crust, we have the data given in Table XX.

As Table XX shows, d was found to be 35 km from the 1·4-th harmonics, while the same was found to be 42 km from the 2·8-th harmonics. Thus the most probable thickness of the earth's crust here is about 40 km. If Meinesz had taken 40 km instead of 25 km in his isostatic reductions, the isostatic anomalies would have been still smaller. The thickness of the earth's crust must here be somewhat smaller than the normal value, because of the mass compensating the negative

Table XX.

	$m=1\cdot4$		$m=2\cdot8$	
	B_m in mgal	H'_m in m	B_m	H_m
	− 86·8	1188	75·3	−276
	−163·0	1711	−83·5	783
	−126·5	855	−72·6	660
	− 83·2	674	−62·8	783
	−108·5	1158	− 3·4	960
	−134·4	1655		
Most Probable d in circular measure	0·131		0·157	
Most Probable d in km	35		42	

average height, which is −1·9 km. If we take the difference of the densities of the crustal and subcrustal materials to be 0·6, the thinning of the earth's crust on account of this will amount to about 9 km. The thickness of the isostatic earth's crust corresponding to zero height is therefore

$$40+10=50 \text{ km.}$$

While the close agreement of this value with those determined from other data might have been accidental, this will be sufficient to illustrate the feasibility of the present method in interpreting gravity anomalies.

Now, from the Fourier coefficients for $\Delta g''_0$ that were already found, it is possible to construct the relief of the boundary surface between the crustal and subcrustal materials, according to the relation

$$h(x)=\frac{1}{2\pi k^2 \Delta\rho}\sum_m B_m \exp(md)\cos mx\,.$$

In the following calculations, we take

$$\Delta\rho=0\cdot6$$

$$d=35 \text{ km.}$$

The calculated reliefs are shown in Table XXI and Fig. 12.

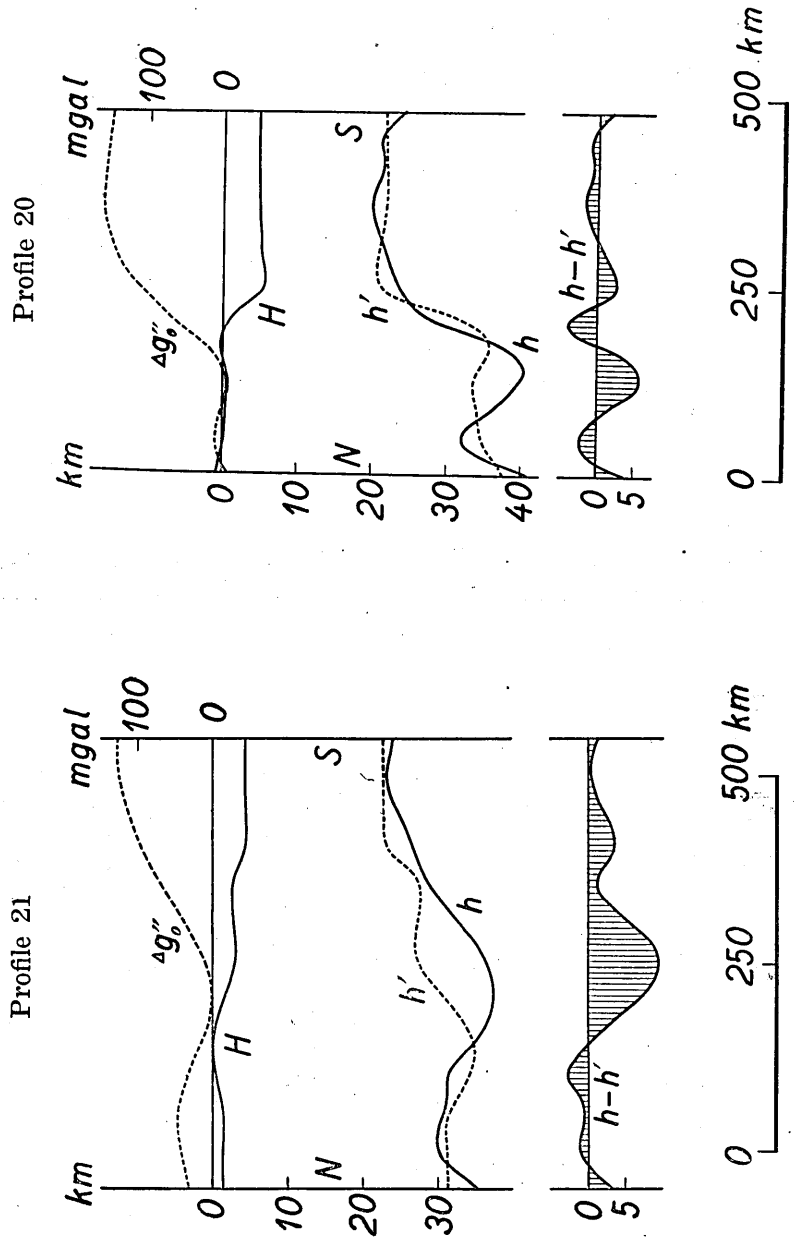

Fig. 12 b.

Fig. 12 a.

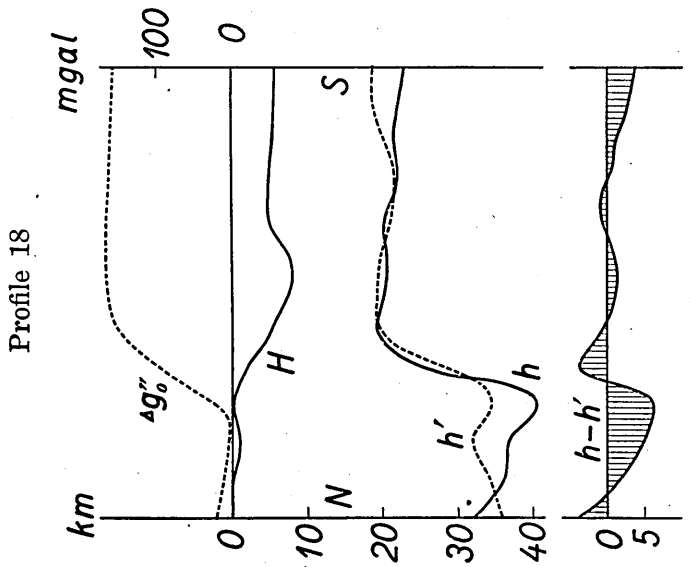

Fig. 12 d.

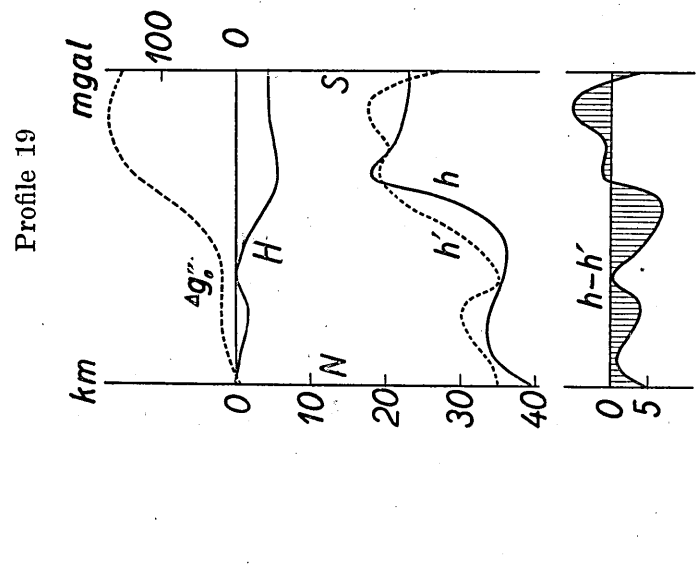

Fig. 12 c.

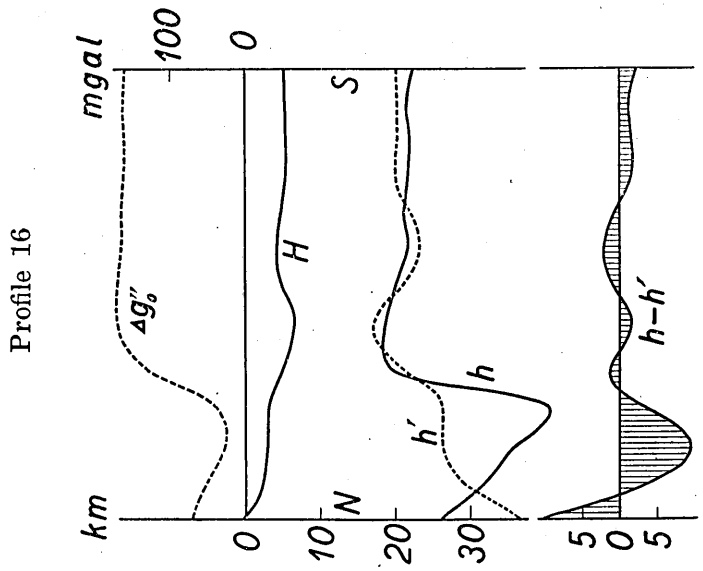

Fig. 12 f.

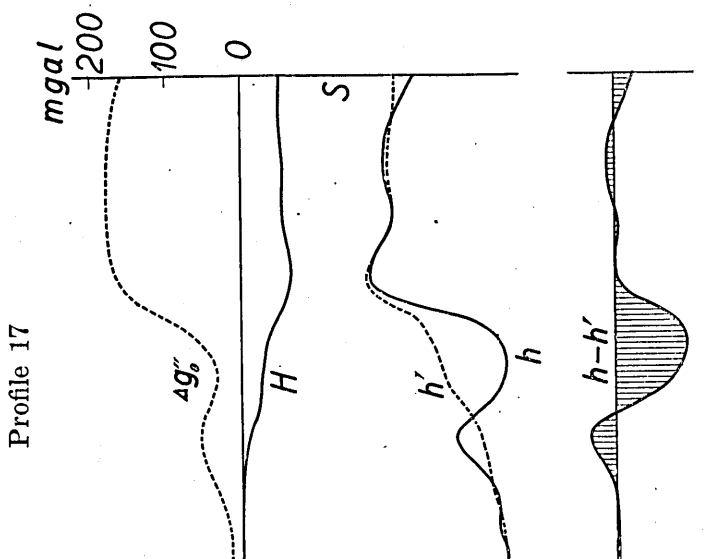

Fig. 12 e.

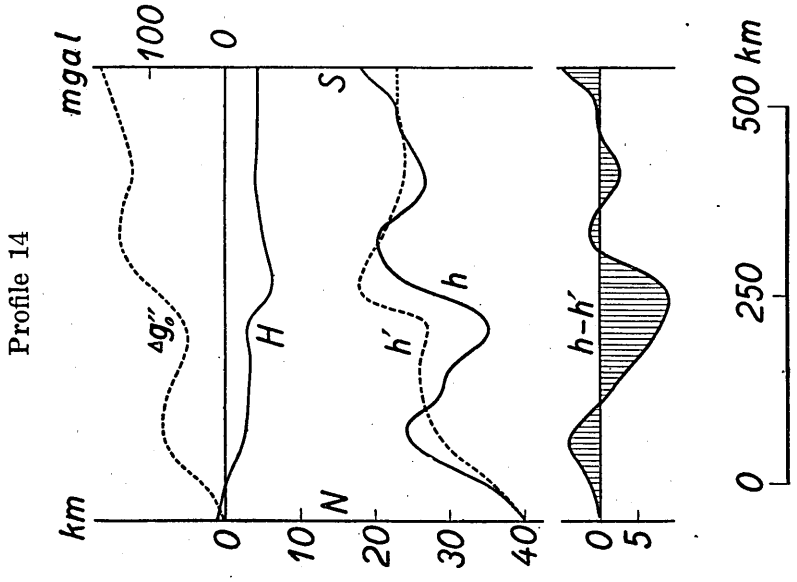

Fig. 13 h

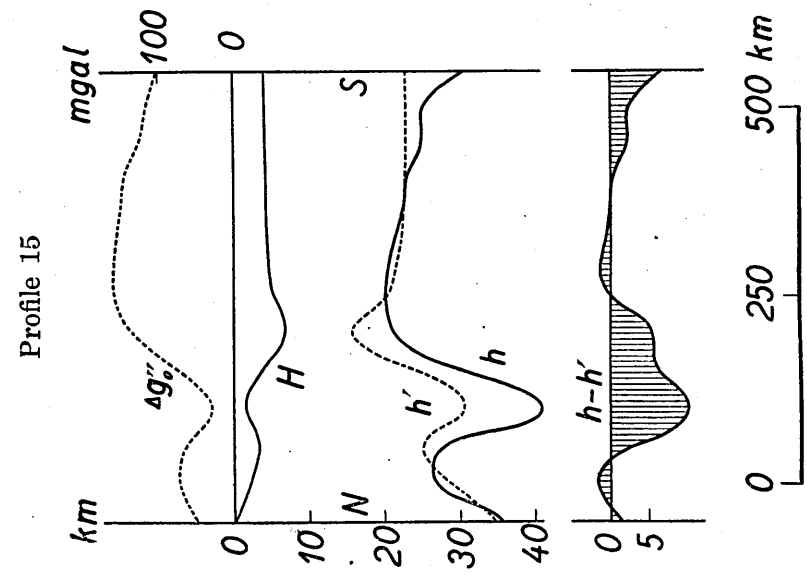

Fig. 13 g.

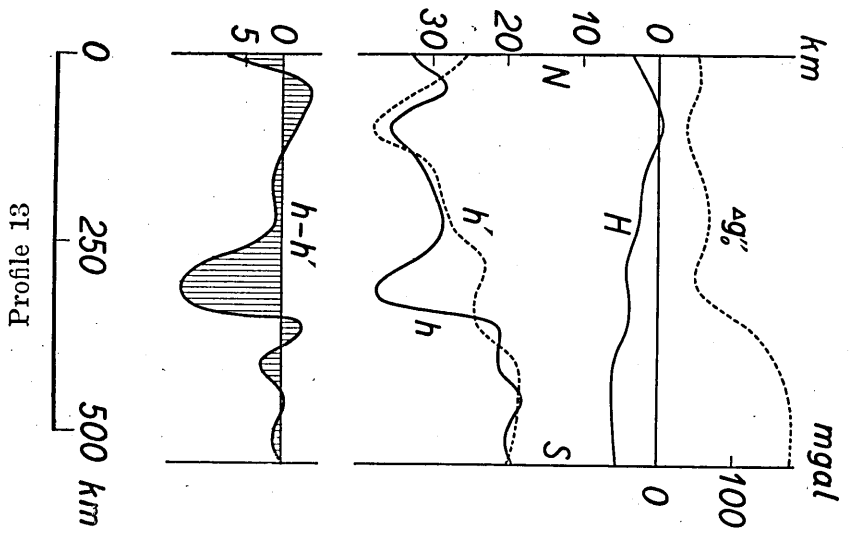

Fig. 13 i.

Table XXI.

Subterranean relief in km.

Profile / x	21	20	19	18	17	16	15	14	13
0	0·3	−6·7	−4·9	2·8	−0·1	8·7	−0·7	−5·3	2·1
1	4·7	2·6	0·5	−1·2	1·2	2·5	7·8	0·9	6 8
2	4·2	−0·5	1·3	−1·6	0·4	−0·8	7·5	9·9	−0·6
3	3·7	−4·2	0·6	−5·7	0·0	−5·9	−5·8	7·5	3·2
4	−0·5	−4·1	−0·2	9·7	1·1	15·3	4·0	5·3	5·2
5	−2·4	5·7	−1·1	15·8	6·2	16·3	13·7	−0·4	6·5
6	−1·3	11·1	0·3	14·8	0·3	15·1	14·9	7·2	2·7
7	1·9	12·8	5·9	14·2	0·8	13·6	14·4	14·6	−2·4
8	6·1	14·0	16·9	14·6	17·6	13·8	12·9	13·3	14·0
9	8·1	15·0	14·7	13·1	15·3	13·4	12·1	8·3	13·7
10	10·4	13·5	16·9	13·5	15·7	13·1	9·9	10·9	17·0
11	11·8	13·9	16·9	13·2	15·2	13·3	9·7	12·0	15·2
12	11·0	10·7	7·6	12·2	11·9	12·4	4·7	17·3	15·3

Table XXII gives the reliefs of the subterranean boundary surface, provided the isostasy is perfect. They were calculated by the relation

$$h = H' \times \frac{2{\cdot}7}{0{\cdot}6}.$$

Table XXII.

Subterranean relief in km if isostasy is perfect.

Profile / x	21	20	19	18	17	16	15	14	13
0	3·6	−2·7	0	−0·9	0·1	−1·4	0·4	−5·0	9·5
1	3·6	0·3	1·4	0·5	0·1	6·3	6·1	−0·7	3·1
2	3·5	0·9	4·0	3·1	0·1	8·6	9·7	5·9	−2·7
3	1·0	1·5	4·5	0·5	0·1	8·7	5·0	8·1	3·3
4	0·4	−0·6	0·2	6·0	1·1	14·0	10·0	9·2	6·4
5	4·0	1·7	1·9	15·2	2·8	17·9	19·1	7·8	7·4
6	8·1	13·4	6·1	15·6	7·1	15·0	14·8	16·7	11·7
7	7·7	14·5	12 8	15·2	10·0	12·0	13·1	15·3	10·9
8	7·2	13·9	15·6	13·9	18·1	12·6	12·4	12·8	11·2
9	11·7	13·4	14·2	13·2	15·6	14·8	12·1	11·1	16·3
10	12·2	13·1	12·8	14·5	15·0	14·7	12·0	11·3	16·5
11	12·2	13·1	12·0	16·0	14·7	14·5	12·0	12·0	16·2
12	12·2	13·1	12·0	16·2	14·4	14·5	12·0	12·0	15·4

Table XXIII gives the differences in the reliefs calculated in these two ways. These correspond to the mass that causes the isostatic gravity anomalies. The results are all shown in Fig. 12, which is self-explanatory.

Table XXIII.

Deviation from isostatic relief in km.

Profile / x	21	20	19	18	17	16	15	14	13
0	−3·3	−4·0	−4·9	3·7	−0·2	10·1	− 1·1	−0·3	− 7·4
1	1·1	2·3	−0·9	−1·7	1·1	3·8	1·7	1·6	3·7
2	0·7	−1·4	−2·7	−4·7	0·3	− 9·4	− 2·2	4·0	2·1
3	2·7	−5·7	−3·9	−6·2	−0·1	−14·6	−10·8	−0·6	− 0·1
4	−0·9	−3·5	−0·4	3·7	0·0	1·3	− 6·0	−3·9	− 1·2
5	−6·4	4·0	−3·0	0·6	3·4	− 1·6	− 5·4	−8·2	− 0·9
6	−9·4	−2·3	−5·8	−0·8	−6·8	0·1	0·1	−9·5	− 9·0
7	−5·8	−1·7	−6·9	−1·0	−9·2	1·6	1·3	−1·3	−13·3
8	−1·1	0·1	1·3	0·7	−0·5	1·2	0·5	0·5	2·8
9	−3·6	1·6	0·5	−0·1	−0·3	− 1·4	0·0	−2·8	− 2·6
10	−1·8	0·4	4·1	−1·0	0·7	− 1·6	− 2·1	−0·4	0·5
11	−0·4	0·8	4·9	−2·8	0·5	− 1·2	− 2·3	0·0	− 1·0
12	−1·2	−2·4	−4·4	−4·0	−2·5	− 2·1	− 7·3	5·3	−0·1

In the present article, no reference was made to the accuracy of the Fourier coefficients used in the calculations, as well as those of

other quantities derived therefrom. They will be discussed in another article to be published later.

In conclusion, the writer acknowledges with thanks the assistance of Mr. T. Fuchida and Miss T. Ayabe in doing much of the numerical computations that are contained in this paper.

---

23. 重力異常と地下構造との關係 (III)

地震研究所 坪 井 忠 二

1) 本論文は，各地で觀測された重力異常を前に提唱した新方法によつて吟味し，それに對する地下構造を論じたものである．

2) R. v. Eötvös が地下構造を假定して計算した重力偏差の値を使つて，逆に其の地下構造を求めて，よい結果を得る事を示した．

3) Africa の Rift Valley で E. C. Bullard が測定した重力異常から地下構造を求めた．

4) 日本の中部地方の重力異常と地形との關係を吟味し，Airy 流の地殻の厚さとして約 50 km を得た．又地方的補償の限界として一邊約 80 km の面積を得た．

5) V. Meinesz が測定した蘭領東印度の重力異常と地形との關係を吟味し，地殻の厚さとして約 50 km，地方的補償の限界として一邊 60 km を得た．又非均衡質量の形を定めた．
